Modeling and Investigation of a Position Control Drive System

Mikho R. Mikhov[1]

Abstract – **The performance of a permanent magnet synchronous motor drive system with position control is discussed in this paper. Detailed study and analysis have been carried out for different loads at respective dynamic and static regimes. The developed computer simulation models and the results obtained can be used in optimizing and tuning of such types of position drive systems.**

Keywords – **Position control drive, Brushless DC motor drive**

I. INTRODUCTION

In recent years permanent magnet synchronous motors (PMSM) have been used in many high performance applications such as numerically controlled machine tools, robotics, electric vehicles, aerospace, and many more [1], [4], [6], [7].

The increasing interest can be explained by their following advantages:

- low power loss and high efficiency;
- high power-mass ratio;
- good heat dissipation characteristics;
- low rotor inertia and good dynamics;
- high speed capabilities.

Generally, according to the phase current waveforms, PMSM electric drives can be classified as brushless DC motor drives (with rectangular current control) and brushless AC motor drives (with sinusoidal current control) [2].

This paper describes the performance of a brushless DC motor drive system with position control in which a parabolic position controller has been applied. Detailed analysis and study by means of modeling and computer simulation have been carried out for the respective transient and steady state regimes. Some investigation results are presented and discussed.

II. MODELING OF THE DRIVE SYSTEM

The simplified block diagram of the position control drive system under consideration is shown in Fig.1. MS is a three-phase PMSM controlled in brushless DC motor mode [5]. The corresponding notations are as follows: PC - position controller; SC - speed controller; RC - reference current block; CC - current controllers block; IC - inverter control block; VI – six-step voltage source inverter; RF – rectifier; PS - position sensor; PF - position feedback block; SF - speed feedback block; L - load of the electric drive; V_{pr} - position reference signal; V_{sr} - speed reference signal; V_{cr} - current reference signals for the phases *a*, *b* and *c* respectively; $2\Delta i_r$ - reference hysteresis band; V_{pf} - position feedback signal; V_{sf} - speed feedback signal; V_{cf} - current feedback signals; V_d - DC link voltage; C - filter capacitor; ω - angular motor speed; θ - angular position; T_l - load torque applied to the motor shaft.

The simplifying assumptions in the analysis of the electric drive are as follows:

- the motor is unsaturated;
- eddy-current and hysteresis effects in the electric motor's magnetic materials have negligible influence on the stator winding current;
- the motor is a symmetrical three-phase machine;
- there is no saliency and therefore self and mutual inductances are constant and independent of rotor position;
- the devices in the power-electronic circuits are ideal.

The PMSM model and the respective power-electronic circuits are represented in Fig. 2, where $S1 \div S6$ are power electronic switches and $D1 \div D6$ are diodes.

The circuit equation in phase variables is:

$$\begin{bmatrix} v_a \\ v_b \\ v_c \end{bmatrix} = \begin{bmatrix} R_s & 0 & 0 \\ 0 & R_s & 0 \\ 0 & 0 & R_s \end{bmatrix} \begin{bmatrix} i_a \\ i_b \\ i_c \end{bmatrix} + \begin{bmatrix} L_a & L_{ba} & L_{ca} \\ L_{ba} & L_b & L_{cb} \\ L_{ca} & L_{cb} & L_c \end{bmatrix} \frac{d}{dt} \begin{bmatrix} i_a \\ i_b \\ i_c \end{bmatrix} + \begin{bmatrix} e_a \\ e_b \\ e_c \end{bmatrix}, \quad (1)$$

where v_a, v_b, v_c are the voltages applied in stator phases *a*, *b* and *c* respectively; i_a, i_b, i_c - the phase currents; e_a, e_b, e_c - the back electromotive forces (EMFs); $R_s = R_a = R_b = R_c$ - the stator phase resistance; L_a, L_b, L_c - the phase self inductances; L_{ba}, L_{ca}, L_{cb} - the mutual inductances.

The back EMF shape waveforms are expressed by the following equation

$$\begin{bmatrix} e_a \\ e_b \\ e_c \end{bmatrix} = \omega \frac{d}{d\theta} \begin{bmatrix} \Phi_a \\ \Phi_b \\ \Phi_c \end{bmatrix}, \quad (2)$$

where Φ_a, Φ_b, Φ_c are the stator magnetic fluxes of phases *a*, *b*, and *c* respectively.

Assuming there is no change in the rotor reluctance with angular position, then

$$L_a = L_b = L_c = L \quad (3)$$

[1]Mikho R. Mikhov is with the Faculty of Automatics, Technical University of Sofia, 8 Kliment Ohridski Str., 1797 Sofia, Bulgaria, E-mail: mikhov@tu-sofia.bg

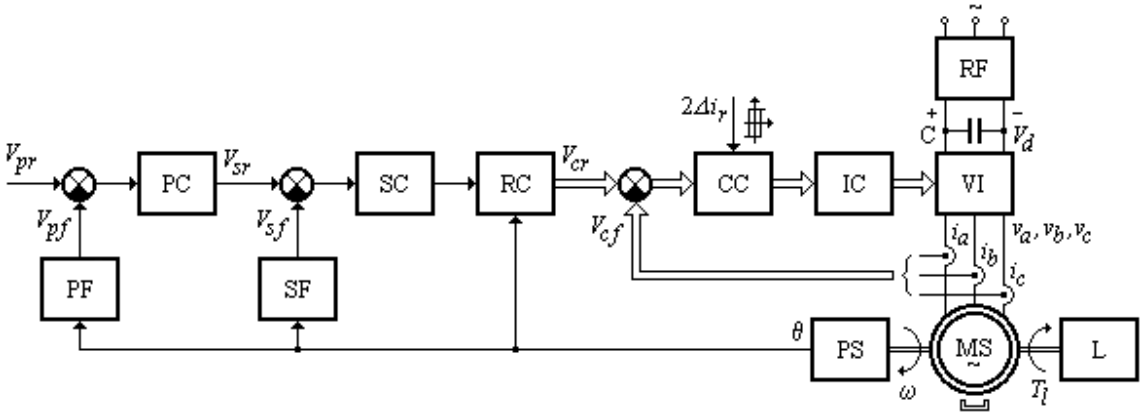

Fig. 1. Block diagram of the drive system under consideration

and

$$L_{ba} = L_{ca} = L_{cb} = M \,. \tag{4}$$

Since the motor windings are star connected, the next relations can be obtained:

$$i_a + i_b + i_c = 0 \,, \tag{5}$$

and

$$Mi_b + Mi_c = -Mi_a \,. \tag{6}$$

Thus, the electric dynamic equations for each motor phase are arranged as follow:

$$\frac{di_a}{dt} = \frac{1}{L_s}\left(v_a - R_s i_a - e_a\right); \tag{7}$$

$$\frac{di_b}{dt} = \frac{1}{L_s}\left(v_b - R_s i_b - e_b\right); \tag{8}$$

$$\frac{di_c}{dt} = \frac{1}{L_s}\left(v_c - R_s i_c - e_c\right), \tag{9}$$

where $L_s = L - M$ is the stator phase inductance.

The motor electromagnetic torque can be expressed as

$$T = \frac{e_a i_a + e_b i_b + e_c i_c}{\omega} \,, \tag{10}$$

and the mechanical dynamics equations are as follows:

$$J\frac{d\omega}{dt} = T - T_l - D\omega \,; \tag{11}$$

$$\frac{d\theta}{dt} = \omega \,, \tag{12}$$

where J is the total inertia referred to the motor shaft; D - the viscous damping coefficient.

The current controllers have programmable hysteresis band $2\Delta i_r$ which determines the modulation frequency of the inverter f_m.

The transfer function of the speed controller is

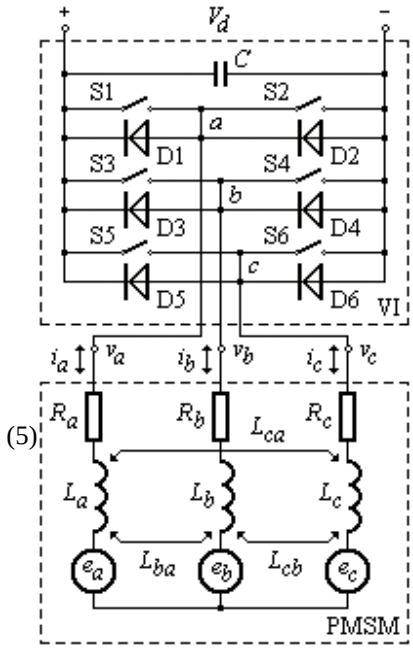

Fig. 2. Model of the motor and respective power-electronic circuits

$$G_{sc}(s) = K_{sc}\left(1 + \frac{1}{\tau_{sc} s}\right), \tag{13}$$

where K_{sc} is the respective coefficient and τ_{sc} is the controller time-constant.

A parabolic position controller is used in the investigated system [3]:

$$G_{pc}(s) = K_{pc}(\Delta\theta) = \frac{K_{sf}}{K_{pf}}\sqrt{\frac{\varepsilon_b}{2\Delta\theta}} \tag{14}$$

where K_{sf} is the coefficient of the speed feedback block; K_{pf} - the coefficient of the position feedback block; ε_b - the

reference deceleration.

The position controller performance is illustrated in Fig. 3, where the following notations are used: $\Delta\theta_{b\max}$ - maximum braking angle; $\Delta\theta_{bs}$ - braking distance at which the controller coefficient value is switched over; $V_{sr\max}$ - maximum speed reference signal.

The motor speed reference signal is determined by the expression

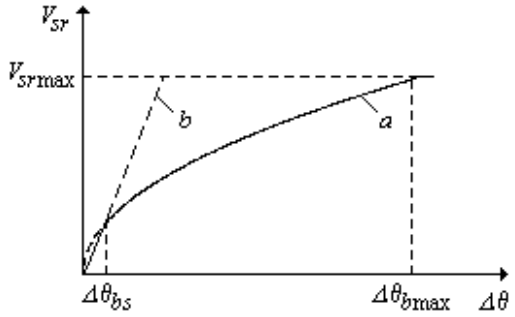

Fig. 3. Illustration of the position controller performance

$$V_{sr} = K_{pc}(\Delta\theta)K_{pf}\Delta\theta \tag{15}$$

After substitution of Eq. 14 in Eq. 15, the following is obtained (Fig. 3, curve *a*):

$$V_{sr} = K_{sf}\sqrt{\frac{\varepsilon_b \Delta\theta}{2}} \tag{16}$$

Reduction of $\Delta\theta$ brings about to increase of K_{pc} up to a value equal to K_{pcs}, calculated according to the admissible overshoot. At $\Delta\theta < \Delta\theta_{bs}$ the $V_{sr}(\Delta\theta)$ ratio coincides with the *b* straight line.

Using MATLAB/SIMULINK software package a number of computer simulation models of electric drives have been developed. A detailed study of the drive system under consideration has been carried out for different loads at transient and steady state regimes.

III. SIMULATION RESULTS

Fig. 4 shows the phase current waveform i_a and the respective trapezoidal back electromotive force e_a obtained at steady state regime for rated load.

Fig 5 illustrates dynamic maintenance of zero phase current.

The programmable hysteresis band influence is shown in Fig. 6 where are represented current waveforms for two reference hysteresis bands.

Fig. 7 represents motor speed stabilization when the load changes. Transient and steady state regimes are represented, as well as the drive system reaction to disturbances expressed in load changes. The load torque acting upon the motor shaft is equal to the rated value $T_{l\text{rat}}$, while the disturbances applied sequentially on the drive are $\pm\Delta T_l = \pm 0.5 T_{l\text{rat}}$. The reference speed is $\omega_r = 157$ rad/s and the starting current is limited to the maximum admissible value $I_{\max}$, which provides maximum starting motor torque.

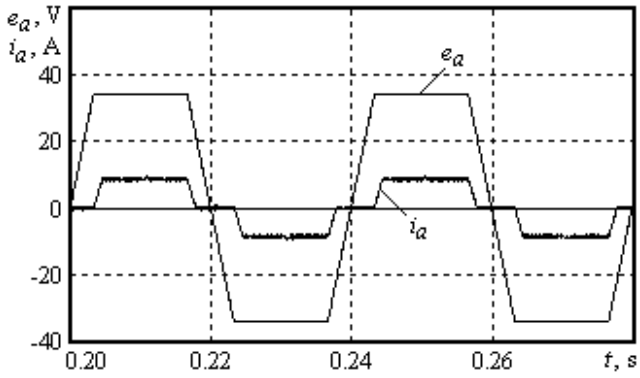

Fig. 4. Phase current and back electromotive force waveforms

Some time-diagrams obtained at reverse speed control with electrical braking are shown in Fig 8. The braking torque of the motor is notated as T_b. The reference speed values in this case are $\pm\omega_r = \pm 100$ rad/s.

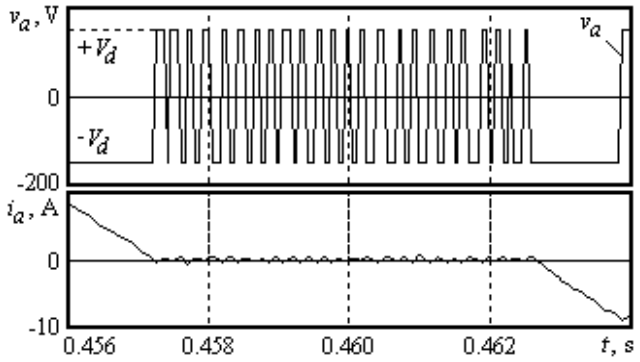

Fig. 5 Dynamic maintenance of zero phase current

Fig. 9 represents simulation results from the investigation of the electric drive system at position control. The motor speed is limited to the maximum value of $\omega_{\max}$, which ensures good dynamics of the drive system.

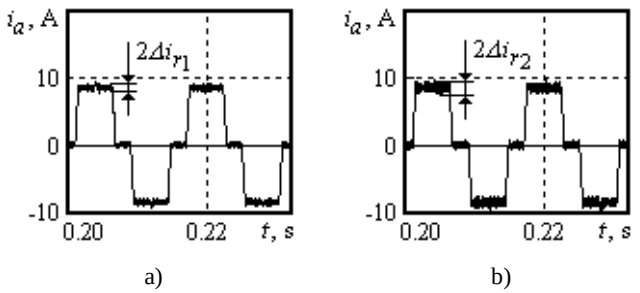

a) b)

Fig. 6. Influence of the current controllers hysteresis band

IV. CONCLUSION

The used motor rated power is $P_{\text{rat}} = 0.6\,\text{kW}$, and the rated speed is $\omega_{\text{rat}} = 157\,\text{rad/s}$.

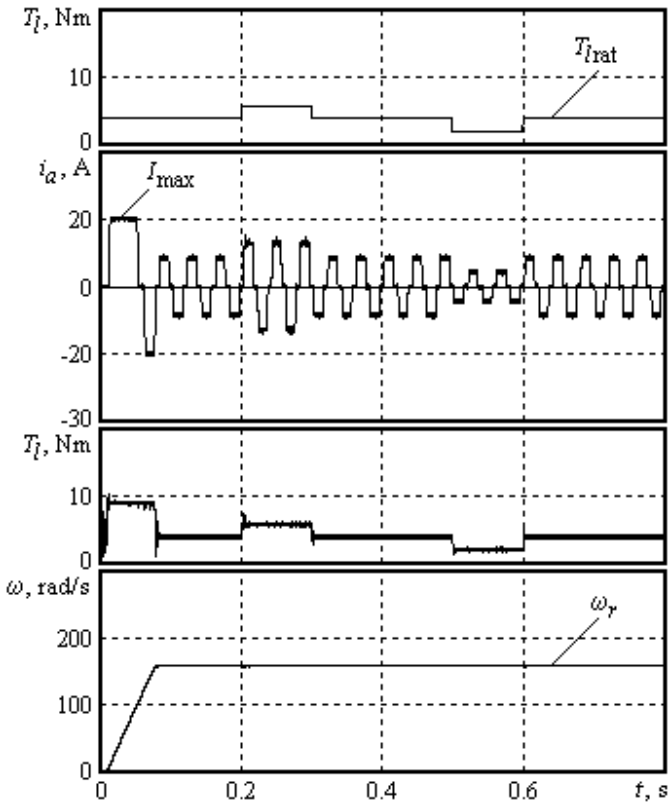

Fig. 7. Motor speed stabilization at load changes

Some specified appropriate setting parameters of the studied electric drive system are as follows: maximum modulation frequency $f_{m\max} = 8\,000\,\text{Hz}$; hysteresis band $2\Delta i_r = 1\,\text{A}$; maximum phase current $I_{\max} = 20\,\text{A}$.

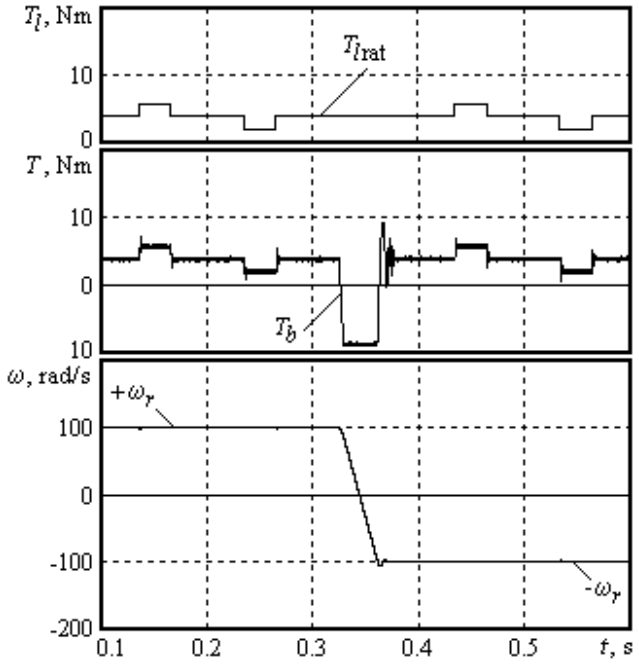

Fig. 8. Diagrams at reverse speed control with electrical braking

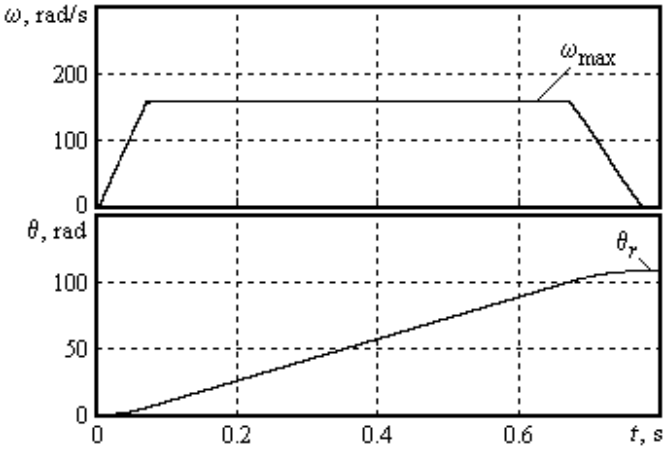

Fig. 9. Time-diagrams at position control of the electric drive

The analysis of the investigated dynamic and steady state regimes shows that the represented electric drive system provides good performance, which makes it suitable for a variety of industrial applications. The developed models and the respective simulation results can be used in optimizing and final tuning of such types of position control drive systems.

ACKNOWLEDGEMENT

This work has been supported by the Bulgarian Ministry of Education and Science, under the project N: 449-8 HK/2004.

REFERENCES

[1] F. Bodin, S. Siala. New reference frame for brushless DC motor drive, *Proceedings of the Conference on Power Electronics and Variable Speed*, pp. 554-559, London, UK, 1998.

[2] I. Boldea, S. A. Nasar, *Electric Drives*, Boca Raton, CRC Press, 1999.

[3] V. I. Klyuchev, *Electric Drive Theory*, Moscow, Energoatomizdat, 1985 (in Russian).

[4] K. Lee, J. Park, H. Yeo, J. Yoo, H. Jo. Current control algorithm to reduce torque ripple in brushless DC motors, *Proceedings of the International Conference on Power Electronics*, pp. 380-385, Seoul, Korea, 1998.

[5] M. R. Mikhov, Investigation of a Permanent Magnet Synchronous Motor Control System, *Technical Ideas*, vol. 38, no. 3-4, pp. 23-34, 2001.

[6] S. K. Safi, P. P. Acarnley, A. G. Jack. Analysis and simulation of the high-speed torque performance of brushless DC motor drives, *IEE Proceedings – Electric Power Applications*, vol. 142, no. 3, pp. 191-200, 1995.

[7] Y. Yoon, D. Kim, T. Lee, Y. Choe, C. Won, A Low Cost Speed Control System of PM Brushless DC Motor Using 2 Hall-Ics, *Proceedings of the International Conference on Mechatronics and Information Technology*, pp. 150-155, Jecheon, Korea, 2003.